Comparison of mathematical models for the dynamics of the Chernivtsi children disease

Dirk Langemann*

Technische Universität Braunschweig, Institute of Computational Mathematics, Pockelsstr. 14, 38106 Braunschweig, Germany.

Igor Nesteruk

National Academy of Science, Institute of Hydromechanics, 8/4 Zheljabova Str., 03057 Kiev, Ukraine.

Jürgen Prestin

Universität zu Lübeck, Institute of Mathematics, Ratzeburger Allee 160, 23562 Lübeck, Germany.

Abstract

Different mathematical models are built of a selection of mechanisms, and they reproduce observations in a quantitatively different manner. A suitable error functional is used to compare the models and to detect mechanisms, which probably caused the observations. For this aim, parameter identification oftentimes is seen as the determination of a best approximation out of the set of feasible solutions of the model, which can be identified with the set. In this paper, the comparison of different model approaches is discussed with respect to observation data from a disease that occurred 1988 in Chernivtsi in Ukraine. The cause of the disease remained unclear. The quantitative measure of the error functional and selected qualitative properties are used to distinguish the models. Even though only a small set of data for the number of affected persons is available, a comparison of a contamination model and an epidemical model suggest that the cause of the disease is rather an infection than an exposure to environmental toxin.

Keywords: model identification, parameter identification, mathematical modeling of infection diseases, SIR model, contamination model
2010 MSC: 93C15, 00A71, 62P10

1. Introduction

All mathematical models, but particularly models for life-science applications, raise the question whether the selection of regarded mechanisms is suitable for the description of the observation under consideration.

In the present paper, we try to identify an appropriate model for realistic given data, which, how oftentimes in life science applications, is available with restrictions only. In general, a first restriction concerns the amount of available data, a second restriction consists in the large error in the data, and a third restriction concerns the distinction between correlation and causal relations. With respect to these restrictions, model selection is a challenging and important task. Here, we map models to their set of feasible solutions, and we discuss classical parameter identification as best approximation within these sets. Then, the mean error of the best approximation is used as criterion to distinguish the models. Since no model will perfectly reproduce measurement data with errors, the comparison addresses rather quantitative than qualitative properties. The comparison may lead to a distinction of models with respect to their ability of reproducing observations.

This distinction technique can be seen in relation to the detection of functional model components which are indispensable for the qualitative reproduction of the observations, cf. [4, 8]. An example for the question which type of model is able to explain a rather complex observation like the plasticity of

*Corresponding author
Email address: d.langemann@tu-bs.de (Dirk Langemann)

date	t_j	A_j	date	t_j	A_j	date	t_j	A_j
5. Aug. 88	1	2	4. Sep. 88	7	9	4. Oct. 88	13	31
10. Aug. 88	2	2	9. Sep. 88	8	10	9. Oct. 88	14	40
15. Aug. 88	3	2	14. Sep. 88	9	12	14. Oct. 88	15	45
20. Aug. 88	4	2	19. Sep. 88	10	12	19. Oct. 88	16	56
25. Aug. 88	5	4	24. Sep. 88	11	17	24. Oct. 88	17	61
30. Aug. 88	6	7	29. Sep. 88	12	19	29. Oct. 88	18	73

Table 1: Cumulative number of children A_j at time instants t_j affected by the severe form of the Chernivtsi children disease.

biochemical systems is investigated in [7]. There, the proof that such behavior is possible was sufficient, but here, in the present paper, we show a comparison between different models, although it is not trivial to apply this comparison technique for more sophisticated models and observations.

In all medical and biochemical applications of mathematical modeling, we are faced to uncertain data which are modeled by hands of a small number of mechanisms, cf. [9]. Also, [17] discusses the question which mechanisms in a model can reproduce selected observations. There is a very broad literature on model selection from philosophical [15, 20], statistical [14], information-theoretic [2] or rather practical view points like the explained variance of a model with uncertain data. In the present article, we deal with an example from life sciences which is regarded to be quite characteristic: On the one hand, we have only a very restricted number of measurements, and providing new measurement data is impossible or very laborious. On the other hand, there are a considerate number of possible mechanisms which affect the data. In addition to the measurement data, qualitative properties of the solutions are known, e. g. monotonicity of positivity conditions, curvature properties or boundedness of solutions.

Since the number of measurements is restricted as oftentimes in life sciences and since the output of models based on ordinary differential equations are rather complicated functions, a full model analysis, e. g. by hands of an information criterion like AIC, does not lead to reasonable results in acceptable time. Here, we compare different hypotheses for models or simply different models. Each of them is based on comprehensible assumptions and leads to a rather simple system of ordinary differential equations. A combination of quantitative and qualitative aspects of the solutions is used to distinguish the models. The qualitative requirements enter the set of feasible solutions of the model, and the quantitative comparison is based on a classical error functional.

The comparison criterion is tested on a disease that occurred 1988 in Chernivtsi in Ukraine, the cause of which is unclear until today. Children younger than 15 years suffered total alopecia, mucosal lesions, hematological, neuro-psychic and cutaneotrophic disordes. This severe form of the disease was accompanied by a larger number of a mild form with partial or local alopecia, and it is unclear whether all these cases are occurrences of the same disease, cf. [22].

The paper is organized as follows. First, the situation and the available data are presented in more detail in Section 2. The following Section 3 introduces different models. These are a simple contamination model, a model of purely exponential growth and the SIR model of the development of an epidemic. Section 4 deals with the discussion of the mathematical comparison technique of different models. Here, the set of feasible solutions of a model is introduced and the classical parameter identification is regarded as best approximation with respect to this set. The solutions of the model equations and their properties are shown in Section 5, and Section 6 compares the presented models. Some further remarks are collected in Section 7. In particular, the mild form of the disease is shortly dealt with here. The paper closes with a short discussion and conclusion.

2. Available information and data

The available data originate from a governmental commission which investigated the disease in October and November 1988, see [22]. At that time, many scientists from the state university and other research institutions in Chernivtsi were trying to find the cause of the disease and the data were widely known. Later, the data were slightly corrected by many authors.

The data used in this paper are presented at 5-day intervals in Table 1 and concern the cases with total alopecia.

Some monthly data were collected for the mild form, too, cf. Figure 3. Let us point out some of the restrictions on the quality of the data. Presumably, it took some time to recognize the autonomy of the disease, so that there might be some particular error in the initial phase. Furthermore, parents who were able to do so, evacuated their children from Chernivtsi into other regions. New cases were partly not registered in a proper way or the information about these cases came with a big delay.

The total numbers of victims varies from 162 to 178 in different reports, cf. [22]. Indeed, one of them reported the last case not until 1994. According to the official reports of the governmental commission, the cause of the disease was reported as a chemical exogenous contamination, although the contaminant substances are not found until now. In [12, 16, 22], the hypothesis of a thallium contamination is discussed. Due to the contamination hypothesis, the diseases was named Chernivtsi chemical disease at that time.

So, Table 1 contains the complete available data on the number of persons affected by the severe form with total alopecia. In particular, it is astonishing that after two cases in the beginning of August, the next cases arose three weeks later. The data on the mild form of the disease are even more insecure. First, the autonomy of this disease is absolutely not clear and a population of 50.000 children in Chernivtsi monthly generates eight to ten sporadic cases of partial or local alopecia by different detailed causes, see [13, 23] for prevalence and duration.

3. Different modeling approaches

Here, we present different mathematical models which will be compared with respect to their ability to reproduce the data given in Table 1. These models are rather simple mathematical models, and they particularly serve as examples for the model comparison and distinction process.

We present three simple models describing different processes. First a contamination model for the disposal of an environmental contaminant at one time instant is given, second a model for a pure exponential growth and third the SIR model for the expansion of an epidemic with possible immunization. All models are given as ordinary differential equations, i. e. local resolution is not taken into account.

3.1. Contamination

The contamination model describes the amount of a toxic substance $G = G(t)$ and the number of victims $V = V(t)$ affected by this substance. We get a two-species model containing differential equations for the decay of the toxic substance and for the influence of the toxic substance to the number of newly affected victims. As usual, we use continuous quantities even for the number of victims, which is to be understood as a rate within a population.

Here, we restrict the model to the case of a unique disposal of the toxic amount G_0 at the time instant t_{init}. Assuming linear relations, we get the model equations, cf. [18]

$$\dot{V} = \beta G, \qquad V(t_{\text{init}}) = 0, \tag{1}$$

$$\dot{G} = -\zeta G, \quad G(t_{\text{init}}) = G_0 \tag{2}$$

for $t \geq t_{\text{init}}$. The parameters are restricted to $\beta \geq 0$ because the effect of the toxic substance should be monotonous in its amount and $\zeta \geq 0$ because the amount of the toxic substance will not increase after the disposal. For time instants $t < t_{\text{init}}$, we set $V(t) = 0$ and $G(t) = 0$.

Eqs. (1), (2) are a contamination model with $m = 4$ parameters, which are combined in the parameter vector $p = (\beta, \zeta, G_0, t_{\text{init}})^{\mathrm{T}} \in \mathbb{R}^3_+ \times \mathbb{R} \subset \mathbb{R}^4$ with $\mathbb{R}_+ = [0, \infty)$. In the present investigation, we count the initial values of the ordinary differential equations in Eqs. (1), (2) as parameters for the resulting cohort of solutions. As a particular case of Eq. (2), $\zeta = 0$ describes a non-decaying toxic substance.

Let us remark that contaminations can be very multifaceted, and numerous processes can be involved in more sophisticated models. Processes like the local dispersal, the transport along some infrastructure or chemical reactions are not at all included in Eqs. (1), (2). Curiously, some contamination events can follow completely different rules, see for instance [5]. There, the harmful dose of the toxic substance was so small that its local dispersal led to a diffusion-like spreading of the disease with an exponentially growing number of victims.

3.2. Exponential growth

Having a look to the increasing tendency of the data given in Table 1, an exponential growth of the number of victims $V = V(t)$ is the assumption used to describe the measurement data. The governing model equation is

$$\dot{V} = \gamma V, \quad V(t_{\text{init}}) = V_0, \tag{3}$$

with the growth rate $\gamma \geq 0$. The initial time instant t_{init} might indicate a starting point of the growth with the initial amount V_0. Eq. (3) describes general self-exciting growth processes, the initial phase of an infection, the unrestricted growth of a population and a lot of other processes more.

The resulting model can be regarded as having three parameters γ, t_{init} and V_0. On the other hand, it is an autonomous differential equation, and the initial time t_{init} does not indicate any particular event. Therefore, we set $t_{\text{init}} = 0$ without loss of generality, and we get the parameter vector $p = (\gamma, V_0)^{\mathrm{T}} \in \mathbb{R}^2_+$ with the number $m = 2$ of parameters. Particularly, we use this model for comparison purposes.

3.3. Epidemic model

The third model under discussion is the classical SIR model for the expansion of an epidemic, see [10]. Here, a population of size N of potential, current or former ill persons is divided into the three compartments $S = S(t)$ of susceptible persons for the disease, $I = I(t)$ of presently infected persons and the number $R = R(t)$ of removed, e. g. immunized, persons. The infection rate $\alpha \geq 0$ and the immunization rate $\varrho \geq 0$ lead to the model equations

$$\begin{aligned} \dot{S} &= -\alpha SI, & S(t_{\text{init}}) = S_0, & \quad (4)\\ \dot{I} &= \alpha SI - \varrho I, & I(t_{\text{init}}) = I_0, & \quad (5)\\ \dot{R} &= \varrho I, & R(t_{\text{init}}) = R_0. & \quad (6) \end{aligned}$$

Adding all equations yields $N = S(t) + I(t) + R(t) = S_0 + I_0 + R_0$. Here, the removed and the currently ill persons build the amount of victims $V = I + R$. Let us remark, that Eq. (6) does not feed back to the governing equations for S and I. So, already Eqs. (4), (5) can be regarded as the entire SIR model.

Eqs. (4), (5), (6) form a model with $m = 6$ parameters and the parameter vector $p = (\alpha, \varrho, S_0, I_0, R_0, t_{\text{init}})^{\mathrm{T}} \in \mathbb{R}^5_+ \times \mathbb{R}$. As an autonomous system of ordinary differential equations with Lipschitz continuous right-hand side the solution can be retrogradely prolongated in a unique manner. Hence, the initial time instant t_{init} is redundant, and the number of parameters can be reduced to five. Doing this, $R(t_{\text{init}}) = 0$ implies $R(t) < 0$ for $t < t_{\text{init}}$ and it becomes necessary to allow $R_0 < 0$ which appears to be unrealistic.

An interesting special case is found by the assumption that the epidemic starts with a single ill person what would mean $I_0 = 1$. If additionally, none already immunized persons are supposed, then $R_0 = 0$ and consequently $S_0 = N - 1$. Under these assumptions, the number of parameters restricts to $m = 4$, which are α, ϱ, S_0 and t_{init}. We will discuss this restriction in Sec. 6 although we know that the SIR model is made for rates S/N, I/N and R/N of the population and large N. The SIR model is not appropriate for small numbers of infected persons because then, stochastic effects dominate the infection process.

The SIR model contains a sub-model for $\varrho = 0$, which is just the logistic growth. Then, $R(t) = R_0$ is constant, and Eqs. (4), (5), (6) reduce to

$$\begin{aligned} \dot{S} &= -\alpha SI, & S(0) = S_0, & \quad (7)\\ \dot{I} &= \alpha SI, & I(0) = I_0, & \quad (8) \end{aligned}$$

with $V = I + R_0$ and $N - R_0 = S(t) + I(t) = S_0 + I_0$. Since $S(t) \geq 0$ and $I(t) \geq 0$ holds true for all t and the system is autonomous, the initial time t_{init} is redundant. The three-parameter model (7,8) can be written as

$$\dot{I} = \alpha(N_0 - I)I = \alpha N_0 \frac{N_0 - I}{N_0} I, \quad I(0) = I_0 \tag{9}$$

with the parameters α, $N_0 = N - R_0$ and I_0. Of course, in some applications, N and R_0 might be counted as different parameters.

For $N_0 \to \infty$ while $\gamma = \alpha N_0$ is fixed, Eq. (9) tends to the exponential growth and so its solution does, cf. Sec. 5. Nevertheless, Eq. (3) is not a special case of Eq. (9) because no $N \in \mathbb{R}$ and no $N_0 \in \mathbb{R}$ lead to a pure exponential growth for the number of victims $V = I(t) + R(t)$. But Eq. (3) is a limit case of Eq. (9) for infinitely increasing N and N_0.

4. Model comparison and distinction

Each of the above models defines possible solutions $V = V(t;p)$ depending on a parameter vector $p \in \mathcal{P}$ out of a set $\mathcal{P} \subseteq \mathbb{R}^m$ of admissible parameters. The set of possible solutions is called the set of feasible functions on the observation interval $[0,T]$. We use a fixed observation interval to compare the data with the model output on the one hand and different models to each other on the other hand. Therefore, all time instants $t_j \in [0,T]$ of the observed data should be inside the interval $[0,T]$. In the situation, where the model contains an initial time $t_{\text{init}} > 0$, the model output $V = V(t,p)$ for $t \geq t_{\text{init}}$ is expanded for $t < t_{\text{init}}$ onto the entire observation interval $[0,T]$. Now, the set of feasible functions is denoted by

$$\mathcal{W} = \mathcal{W}(\mathcal{P}) = \{V = V(t;p) : p \in \mathcal{P} \subseteq \mathbb{R}^m\} \subseteq C([0,T]). \tag{10}$$

The selection of mechanisms occurring in the model, determines the set of feasible functions. On a technical level, a model containig uncertain or unknown parameters, can be identified with the set $\mathcal{W}$.

The set of feasible functions $\mathcal{W}$ is assumed as a subset of all continuous functions. This holds true for the above models. In other cases, a more general function space, e. g. the space of piecewise continuous function is thinkable without any additional problems.

We denote the set of available measurement data $A = \{(t_j, A_j) : j = 1, \ldots, n\}$. We introduce a general distance concept $d(V,A)$ between a function $V \in C([0,T])$ and the set of available data. Then, parameter identification is the minimization of an error functional like $J = d(V,A)^2$, i. e. the minimization of the squared distance between the solution $V = V(\cdot;p) \in \mathcal{W}$ and the given set of data. We get

$$J_{\min}(\mathcal{W}) = \min_{V \in \mathcal{W}} d(V,A)^2 = \min_{p \in \mathcal{P}} d(V(\cdot,p),A)^2. \tag{11}$$

Since, we measure the distance between a function space and a set of data, we use the well-defined projection $\Pi : C([0,T]) \to \mathbb{R}^n$ acting as $f \mapsto (f(t_j))_{j=1}^n = \Pi f$. Oftentimes, the distance concept of the mean squared error

$$J = d(V,A)^2 = \sum_{j=1}^{n} \left(V(t_j,p) - A_j\right)^2 = \|\Pi V(\cdot;p) - (A_j)_{j=1}^n\|_2^2 \tag{12}$$

is used as error functional, which coincides with the maximum-likelihood function in stochastics if the measurements are regarded as independent, identically distributed random variables. In practical applications, we are used to write the error functional $J = J(p)$ depending on the parameter vector, and by the use of Eq. (11), the parameter identification reads as minimization

$$J_{\min}(\mathcal{W}) = \min_{p \in \mathcal{P}} J(p) = \min_{p \in \mathcal{P}} \sum_{j=1}^{n} \left(V(t_j;p) - A_j\right)^2. \tag{13}$$

A parameter vector $p_{\min}$ fulfilling $J(p_{\min}) = J_{\min}$ is seen as optimal parameter vector within the set $\mathcal{P}$. The respective function $V = V(\cdot, p_{\min})$ can be regarded as a best-approximation or a best-fitting function for the set of data A within the set of feasible functions $\mathcal{W}$ and thus for the present model.

It is obvious that the error functional and thus also its minimum depend on the chosen distance concept and on the set of feasible functions. In particular, the optimal parameter vector $p_{\min}$ might depend sensitively on the chosen parameter set $\mathcal{P}$. The parameter vector and the respective feasible function are only optimal within $\mathcal{P}$ or $\mathcal{W}$, respectively. Finally, let us denote the mean error as

$$s(\mathcal{W}) = \sqrt{\frac{J_{\min}(\mathcal{W})}{n-1}}$$

in analogy to the estimation of the mean deviation in stochastics.

Different models generate different sets of feasible functions. A purely quantitative opportunity to compare the models consists in the comparison of the mean errors. If $s(\mathcal{W}_1) < s(\mathcal{W}_2)$, then the set of data A lies closer to the function set $\mathcal{W}_1$ than to $\mathcal{W}_2$, and thus, the model M_1 generating $\mathcal{W}_1$ is more appropriate to describe the data A than the model M_2 generating $\mathcal{W}_2$. We can say that it is more probable that the data were extracted from a process governed by the model equations M_1 than by the model equations M_2. We should remark that this assertion is not very strong for large mean errors when both models are far away from reproducing the data in a visually acceptable manner.

A model extension M_2 of the model M_1 is an extension of the set of feasible functions, maybe by an extension of the parameter set $\mathcal{P}$ or even of the length of the parameter vector. In the latter case, the original model should be a special case of the extended model. In both cases, $\mathcal{W}_1 \subseteq \mathcal{W}_2$ holds true, and $s(\mathcal{W}_2) \leq s(\mathcal{W}_1)$ is a trivial consequence. Every model extension diminishes the optimal error functional $J_{\min}$. The amount of reduction can be regarded as an opportunity to quantify the improvement by the model extension.

Again, we should remark that $J_{\min}(C([0,T])) = 0$ whenever $t_i \neq t_j$ for $i \neq j$. In this case, we get a pure interpolation of the data, which usually does not give any insight in the underlying process. Therefore, the space $C([0,T])$ itself is not regarded as a set of feasible functions of a model.

In addition of the purely quantitative mean error, qualitative properties of the feasible functions, e. g. curvature properties, positivity conditions or the long-term behavior, can be used to compare models. In this article, we will mainly use the mean error $s(\mathcal{W})$ to compare the three models from Sec. 3 in Sec. 6 after having described the sets of feasible functions in the following section.

5. Sets of feasible functions of different models

Here, we identify the sets of feasible functions of the different modeling approaches. The models of contamination of pure exponential growth allow to give analytically closed descriptions of the set of feasible functions $\mathcal{W}_{\text{tox}}$ of Eqs. (1), (2) and of the set of feasible functions $\mathcal{W}_{\text{exp}}$ of Eq. (3). There is no analytically closed form of the solutions of the SIR model. Therefore, we deal with numerical solutions in this case, and we give several forms of approximative solutions. Furthermore, we collect some properties of the feasible functions in this section.

Let us mention that we will compare the model output V on the observation interval $[0,T]$ with the measurement data A_j at the time instants $t_j \in [0,T]$. But, some formulations of the model equations contain the initial time instant t_{init}, when the modeled process is regarded to start. For comparison of the model output with the data and of the different models to each other, we retrogradely expand the solutions of the model equations for $t < t_{\text{init}}$, too.

5.1. Contamination model

In the case $\zeta > 0$, the solution of Eqs. (1), (2) for $t \geq t_{\text{init}}$, i. e. after the unique dispersal of the toxic substance, is

$$G(t) = G_0 \mathrm{e}^{-\zeta(t-t_{\text{init}})}, \quad V(t) = \frac{\beta G_0}{\zeta}\left(1 - \mathrm{e}^{-\zeta(t-t_{\text{init}})}\right). \tag{14}$$

The settings $G(t) = 0$ and $V(t) = 0$ for $t < t_{\text{init}}$ lead to a jump in G at $t = t_{\text{init}}$, but we get a continuous function $V \in C([0,T])$ on the observation interval. As already said in Sec. 3.1, the parameter vector of the feasible functions is $p = (\beta, \zeta, G_0, t_{\text{init}}) \in \mathcal{P} = \mathbb{R}_+^3 \times \mathbb{R}$. The restriction $\zeta > 0$ leads to the parameter space $\tilde{\mathcal{P}} = \mathbb{R}_+ \times (0,\infty) \times \mathbb{R}_+ \times \mathbb{R} \subset \mathcal{P}$. Now, the set of feasible functions with $\zeta > 0$ reads as

$$\tilde{\mathcal{W}}_{\text{tox}} = \left\{ V = V(t;p) = \frac{\beta G_0}{\zeta}\left(1 - \mathrm{e}^{-\zeta(t-t_{\text{init}})}\right) H(t - t_{\text{init}}) : p \in \tilde{\mathcal{P}} \right\} \subset C([0,T])$$

using the Heaviside function $H = H(t)$. The curvature of all $V \in \tilde{\mathcal{W}}_{\text{tox}}$ fulfills

$$V''(t) = -\beta\zeta G_0 \mathrm{e}^{-\zeta(t-t_{\text{init}})} \leq 0 \quad \text{for all} \quad t > t_{\text{init}}$$

and the limit behavior for large t is

$$\lim_{t\to\infty} V(t) = \frac{\beta G_0}{\zeta} = V_\infty. \tag{15}$$

Very small parameters ζ allow to use the Taylor-expansion for the exponential term in Eq. (14), and with the abbreviation $\eta = \beta G_0$, we get

$$V(t) = \eta(t - t_{\text{init}}) + \mathcal{O}(\zeta T) \quad \text{for} \quad t \in [t_{\text{init}}, T].$$

For $\zeta \to 0$, the function $V(t)$ tends to the solution of Eqs. (1), (2) for $\zeta = 0$, i. e. for the limit case of a non-decaying toxic substance, which means $G(t) = G_0$ and the linear growth $V(t) = \eta(t - t_{\text{init}})$. By the way, $\zeta \to 0$ causes $V_\infty \to \infty$ because of Eq. (15). Now, the set of all feasible functions is

$$\mathcal{W}_{\text{tox}} = \tilde{\mathcal{W}}_{\text{tox}} \cup \left\{ V(t;p) = \beta G_0 \cdot (t - t_{\text{init}}) H(t - t_{\text{init}}) : p \in \mathcal{P} \backslash \tilde{\mathcal{P}} \right\}.$$

5.2. Model of pure exponential growth

The solution of Eq. (3) simply is $V(t) = V_0 \mathrm{e}^{\gamma(t-t_{\mathrm{init}})}$. The solution can be retrogradely prolongated for $t < t_{\mathrm{init}}$, too. Again, we fix the observation interval, and we use $V \in C([0,T])$. The set of feasible functions can be written as

$$\mathcal{W}_{\mathrm{exp}} = \left\{ V(t;p) = V_0 \mathrm{e}^{\gamma(t-t_{\mathrm{init}})} : p = (\gamma, V_0, t_{\mathrm{init}})^{\mathrm{T}} \in \mathbb{R}_+^2 \times \mathbb{R} \right\} \subset C([0,T]) \tag{16}$$

or using the autonomy property of Eq. (3) as

$$\mathcal{W}_{\mathrm{exp}} = \left\{ V(t;p) = V_0 \mathrm{e}^{\gamma t} : p = (\gamma, V_0)^{\mathrm{T}} \in \mathbb{R}_+ \times \mathbb{R} \right\} \subset C([0,T]). \tag{17}$$

As already mentioned in Sec. 3.2, the set $\mathcal{W}_{\mathrm{exp}}$ can be parametrized by two parameters $p = (\gamma, V_0)$ with $p \in \mathcal{P} = \mathbb{R}_+ \times \mathbb{R} \subset \mathbb{R}^2$ or in a redundant description with three parameters including the initial time t_{init}. Here the curvature fulfills

$$V''(t) = \gamma^2 V_0 \mathrm{e}^{\gamma t} \geq 0 \quad \text{for all} \quad t \in [0,T]$$

for all feasible functions $V \in \mathcal{W}_{\mathrm{exp}}$. Furthermore, $V''(t) > 0$ for $\gamma > 0$, and $V(t)$ tends to infinity for $\gamma > 0$ whenever t increases over all bounds.

5.3. SIR model of an epidemic

Since no explicit solution of the SIR model equations in Eqs. (4), (5), (6) is available in a closed analytical form, cf. [1], we search for relations and approximations for the quantities. Here, we use the model equations including the redundant t_{init} to show its occurrence in the approximations. First like in [6, 10, 6], Eq. (5) is divided by Eq. (4) and the relative immunization rate $\mu = \varrho/\alpha$ is introduced. An integration with respect to S results in the relation

$$I(t) + S(t) - \mu \ln S(t) = I_0 + S_0 - \mu \ln S_0 = C \quad \text{for all} \quad t \geq t_{\mathrm{init}}. \tag{18}$$

That means that $I = I(S) = C - S + \mu \ln S$ is maximal for $S = \mu$, which is the threshold for an epidemic situation. Since S is monotonously decreasing and there are not any non-trivial stationary points of Eqs. (4), (5), (6), we get

$$\lim_{t\to\infty} I(t) = 0 \quad \text{and} \quad S_\infty = \lim_{t\to\infty} S(t) \quad \text{with} \quad S_\infty + \mu \ln S_\infty = C.$$

Interestingly, we can derive an ordinary differential equation for the monotonously increasing number of victims $V = I + R = N - S$, which is the quantity, we have measurement data A_j for, cf. Table 1. Adding Eq. (4) and Eq. (5) gives $\dot{V} = \alpha S I$. Eq. (18) reads as $I = I_0 + S_0 - S + \mu(\ln S - \ln S_0)$ with $I_0 + S_0 - S = N - R_0 - S = V - R_0$, and we finally get the ordinary differential equation

$$\dot{V} = \alpha(N - V)\left(V - R_0 + \mu \ln \frac{N - V}{S_0} \right) \quad \text{with} \quad V(0) = V_0 = I_0 + R_0. \tag{19}$$

for $V = V(t)$. Separation of variables yields

$$F(V; \mu, S_0, I_0, R_0, t_{\mathrm{init}}) = \int_{V_0}^{V} \frac{\mathrm{d}v}{(N - v)\left(v - R_0 + \mu \ln \frac{N-v}{S_0} \right)} = \alpha(t - t_{\mathrm{init}}). \tag{20}$$

Eq. (20) provides a unique time $t \geq t_{\mathrm{init}}$ for every $V \geq V_0$ and every choice of parameters. Having $V = V(t)$, Eq. (18) with $S = N - V$ gives $I = I(t)$ and finally $R = V - I$ is found.

The set $\mathcal{W}_{\mathrm{sir}}$ of feasible functions of the SIR model is formed by all functions $V = V(t)$ fulfilling Eq. (20), i. e. by all $V = I + R$ where $I = I(t)$ and $R = R(t)$ are solutions of the system of Eqs. (4), (5), (6) for parameters $p = (\alpha, \varrho, S_0, I_0, R_0, t_{\mathrm{init}})^{\mathrm{T}}$ with $p \in \mathcal{P} = \mathbb{R}_+^5 \times \mathbb{R} \subset \mathbb{R}^6$. The six parameters of $\mathcal{W}_{\mathrm{sir}}$ can be reduced by fixing $t_{\mathrm{init}} = 0$ to five parameters because the system of ordinary differential equations (4), (5), (6) is autonomous with a right-hand side, which is Lipschitz continuous, and thus, it can be solved in backward time direction. Since then, $R(t)$ does not stay necessarily positive, negative R_0 are to be allowed. An explicit description of the modified parameter set is a rather technical aspect because the existence of a $t_{\mathrm{init}} \in [0,T]$ with a non-negative $R(t_{\mathrm{init}})$ is a reasonable requirement for a realistic behavior of the SIR model.

We remark that a solution $(S(t), I(t), R(t))$ of Eqs. (4), (5), (6) transforms $R_{\mathrm{n}}(t) = R(t) - R_0$ into a solution $(S(t), I(t), R_{\mathrm{n}}(t))$ of the SIR system with $R_{\mathrm{n}}(t_{\mathrm{init}}) = 0$. Therefore, a vanishing initial condition for R is oftentimes seen as standard.

First, we approximate the solution of Eq. (20) for the case $R_0 = 0$ and for a large population size compared to the number of victims, i. e. $N \gg V \geq v \geq V_0$. With $S_0 = N - V_0$, the approximations

$$\frac{1}{N-v} = \frac{1}{N} + \mathcal{O}\left(\frac{V}{N}\right) \quad \text{and} \quad \ln\frac{N-v}{S_0} = \ln\left(1 + \frac{V_0 - v}{N - V_0}\right) = \ln 1 + \mathcal{O}\left(\frac{V}{N}\right)$$

yield

$$F = \int_{V_0}^{V} \frac{\mathrm{d}v}{Nv} + \mathcal{O}\left(\frac{V}{N}\right) = \frac{1}{N}\ln\frac{V}{V_0} + \mathcal{O}\left(\frac{V}{N}\right) = \alpha(t - t_{\mathrm{init}}).$$

Omitting the first order term and fixing $\gamma = N\alpha$ provide just the functions in Eq. (16) of pure exponential growth.

Second, the use of the next Taylor approximation

$$\ln\frac{N-v}{S_0} = \ln\left(1 + \frac{V_0 - v}{N - V_0}\right) = \frac{V_0 - v}{N} + \mathcal{O}\left(\frac{V}{N}\right)^2$$

leads to

$$F = \int_{V_0}^{V} \frac{\mathrm{d}v}{(N-v)\left(v + \mu\frac{V_0 - v}{N}\right)} + \mathcal{O}\left(\frac{V}{N}\right)^2 = \alpha(t - t_{\mathrm{init}}).$$

The solution can be given in the form

$$V(t) = \frac{EN(N-\mu) + \mu V_0}{E - N + \mu} \quad \text{with} \quad E = \frac{V_0 N}{V_0 - N}\mathrm{e}^{\alpha\left(\frac{\mu V_0}{N} + N - \mu\right)(t - t_{\mathrm{init}})}, \tag{21}$$

and it has the saturation property $\lim\limits_{t\to\infty} V(t) = N \in \mathbb{R}$.

We compare this approximation with the solution of the logistic growth for $t_{\mathrm{init}} = 0$ in Eq. (9), which reads with $V = I$ as

$$\int_{V_0}^{V} \frac{\mathrm{d}v}{(N_0 - v)v} = \alpha t \quad \text{with} \quad V(t) = \frac{NV_0\mathrm{e}^{\alpha N t}}{N + V_0(\mathrm{e}^{\alpha N t} - 1)}.$$

The solution of the logistic growth reproduces the saturation property with $\lim\limits_{t\to\infty} V(t) = N$. Again, the parameter $\gamma = \alpha N_0$ is occurring as exponent. The model of logistic growth has inherited this characteristic parameter from the model of pure exponential growth.

6. Results of model comparison

Here, we present some optimization results of the parameter identification. We use the mean error s of the best-fitting function of a model as a quantitative criterion to compare different models. Furthermore, we discuss some qualitative properties of the feasible functions and compare them to the available data.

We emphasize that we do not discuss the optimization method itself here. We refer to [11] for a description of optimization methods. The present optimization problems are sufficiently small to be successfully handled by simple brute search in the initial phase and a steepest-descent method for the refinement.

The best-fitting curves are presented in Fig. 1 for the contamination model, the pure exponential growth and the SIR model for an epidemic. The optimal parameters with respect to the error functional in Eq. (12) are given in the caption.

The left plot gives the best-fitting curve within $\mathcal{W}_{\mathrm{tox}}$ with $J(\mathcal{W}_{\mathrm{tox}}) = 399.8$ and $s(\mathcal{W}_{\mathrm{tox}}) = 4.85$ in the solid line. We can say, that the best-fitting function in the set of all feasible functions of the model has a mean error in the number of victims of nearly 5 cases, which is quite a large amount with respect to the total number of victims.

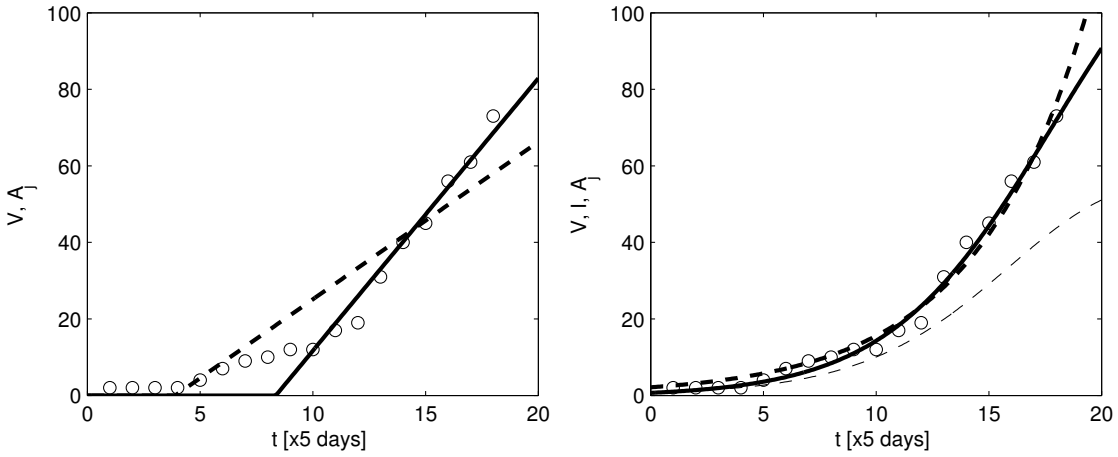

Figure 1: Left: Contamination model. Solid: best-fitting curve $V(t) = \eta(t-t_{\text{init}})H(t-t_{\text{init}})$ with $\eta = \beta G_0 = 7.12$, $t_{\text{init}} = 8.36$ and $s = 4.85$. Dashed line: best-fitting curve $V(t) = \eta(t - t_{\text{init}})$ with $\eta = 4.12$, $t_{\text{init}} = 3.90$ and $s = 7.84$. Right: exponential growth and SIR model. Dashed fat line: best-fitting exponential growth in Eq. (17) with $\gamma = 0.20$, $V_0 = 2.13$ and $s = 2.80$. Solid fat line: best-fitting SIR model in the case $R_0 = 0$ with $N = 160$, $\alpha = 0.0025$, $\varrho = 0.12$, $I_0 = 0.68$ and $s = 2.04$. Dashed thin line: number of infected persons $I = I(t)$ in the SIR model. In both figures, dots represent the number of victims A_j.

Furthermore it is remarkable that $\mathcal{W}_{\text{tox}}$ contains curves with non-positive second derivative whereas the measurement data in Table 1 show a positive curvature. Therefore, it is not astonishing that the best-fitting curve is a line for $t > t_{\text{init}}$. This initial time instant is $t_{\text{init}} = 8.36$, some weeks after the occurrence of the first cases of the disease. This is a strong hint that the contamination model does not realistically reproduce the observations in the data.

For comparison, we show in the left plot of Fig. 1 the best-fitting linear function without restricting the results to non-negative values. This alternative best-approximation has an even larger mean error of $s(\mathcal{W}_{\text{tox}}) = 7.84$ and $t_{\text{init}} = 3.90$. Interestingly, this value could be interpreted as the first time-instant when the number of cases increases above the first two cases at t_1.

The dashed lines in the right plot of Fig. 1 show the best-approximation in $\mathcal{W}_{\text{exp}}$ with $J(\mathcal{W}_{\text{exp}}) = 133.1$ and $s(\mathcal{W}_{\text{exp}}) = 2.80$, and the solid line shows the best-approximation in $\mathcal{W}_{\text{sir}}$ with $J(\mathcal{W}_{\text{sir}}) = 71.1$ and $s(\mathcal{W}_{\text{sir}}) = 2.04$. We remark that the mean error is considerably diminished in comparison with the contamination model. Particularly, the SIR model fits the measurement data with an accuracy, which is very fine relative to other life-science applications. Both curves show the curvature behavior from the data.

If the contamination model, the model of pure exponential growth and the SIR model are compared with respect to their ability to reproduce the measurement data, we find a clear advantage for the exponential growth and the SIR model relative to the contamination model, because

$$4.85 = s(\mathcal{W}_{\text{tox}}) > s(\mathcal{W}_{\text{exp}}) > s(\mathcal{W}_{\text{sir}}) = 2.04. \tag{22}$$

The difference between the best-fitting curves in $\mathcal{W}_{\text{exp}}$ and $\mathcal{W}_{\text{sir}}$ in the interval $[0, T]$ with $T = 20$, where measurement data are available from Table 1, is rather small. There is no intuitive advantage of the SIR model in this interval. Since the pure exponential growth is a limit case of the SIR model, we can regard the SIR model as a model refinement of the pure exponential growth. Nevertheless, the improvement by this model refinement is small. That corresponds to the fact that no data on the removed compartment is available and that the initial phase of the SIR model is dominated by an exponential growth behavior. We remark that the growth rate $\alpha S \leq \gamma$ in the SIR model diminishes with increasing V and that the growth starts on a lower level. Finally, the hypothesis of an infection makes it more probable to have only two initial cases at t_1, and the next cases at t_5 only.

Concerning the ability to predict future behavior of the disease and not only to reproduce the measurement data, we show the long-term behavior of the optimal solutions in Fig. 2. As expected the exponential growth does not show any saturation behavior and $V = V(t)$ grows over all limits whereas the SIR model shows a limit behavior and $V_\infty \approx 158$ which coincides very well with the observed 162 cases with total alopecia, i. e. in the severe form.

Additionally to the SIR model and the pure exponential growth, Fig. 2 contains the best-fitting solution of the SIR model under the restriction of $I_0 = 1$, $R_0 = 0$ for a free initial time, which is computed as

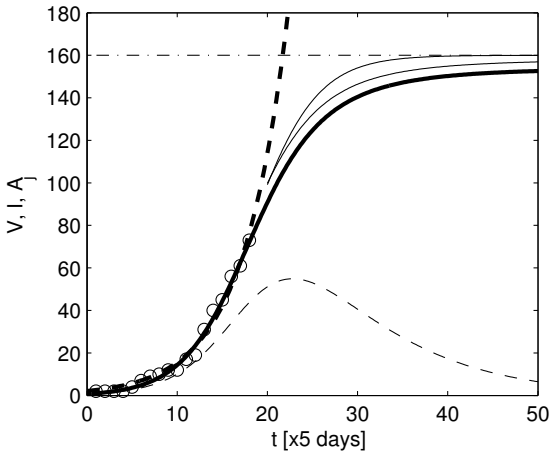

Figure 2: Best fitting curves in a longer time-interval with saturation line $N = 160$. Dashed fat line: exponential growth. Solid fat line: $V(t)$ of the SIR model. Dashed thin line: Infected persons $I(t)$ of the SIR model. Solid thin line: starting from beneath, best-fitting SIR model curve in the case $I_0 = 1$, $R_0 = 0$ with parameter vector $(N, \alpha, \varrho, t_{\text{init}})^{\text{T}}$ with $s = 5.10$ and best-fitting approximation from Eq. (21) with $s = 2.49$.

$t_{\text{init}} = 0.81$. It is obvious that a restriction of $\mathcal{W}_{\text{sir}}$, i. e. a smaller set of feasible functions increases the mean error, and indeed we find $s = 5.10$ in this case. The restriction leads to a larger mean error than the contamination model. So, under this restriction the comparison of both model approaches is balanced. No quantitative decision is possible, even if the qualitative behavior seems to fit better to the data. Finally, the best-fitting approximation from Eq. (21) is shown. Both additional curves are omitted in the plot for $t < 20$ because they are optically undistinguishable from the other curves.

7. Further observations

A logarithmic regression of the data from Table 1 gives the parameters $\gamma = 0.23$, $V_0 = 1.3$ for a solution in $\mathcal{W}_{\text{exp}}$. Then, the mean error is $s = 5.10$, although the linear regression is optimal with respect to an error functional comparing $\ln V(t_j; p)$ and $\ln A_j$, cf. [3]. In such an approach small data values A_j are stronger weighted than larger ones, what does not appear to be the most appropriate choice because we have discussed in Section 2 that small A_j are even more uncertain than large ones. An analogous deviation would occur if parameter identification would be done by minimizing the defect of Eq. (20), which would coincide with a change of the error functional, too. Both approaches reduce to linear regression of changed data and generate impressively high regression coefficients. By the way, even the best-approximating curves for the contamination model do so.

Figure 3 gives the best approximating solutions of the SIR model for the data of the mild form of the Chernivtsi children disease. We see that we get a large mean error, and the behavior of the data is not well reproduced by the best fitting curves. The same observation is conserved even if the mild form and the severe form are considered together. That means that the SIR model is probably not appropriate to reproduce the data including the mild form of the disease. We recall the monthly up to ten sporadic cases, which might have entered the collected data. Furthermore, in the last time instants in Figure 3, a possible second wave of infection may be recognizable, which would need different modeling approaches, see [19].

8. Discussion and conclusion

We have applied different models for the data from the Chernivtsi children disease. We have used a combination of quantitative and qualitative aspects of the solutions to distinguish the models. The quantitative part is the mean error between the model reproduction and the measurement data. The combined criterion is able to distinguish between different models.

We have shown that parameter identification within a fixed model is a special situation of model selection. In both tasks, a best approximating solution is sought in a class of feasible functions. The difference lies in the extension of this class. Thus from the mathematical point of view, model selection

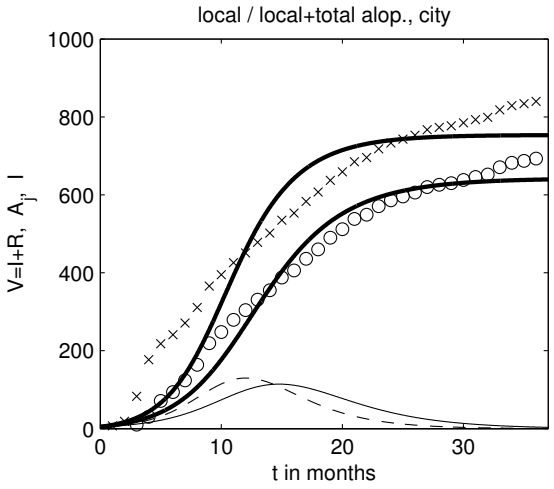

Figure 3: Best fitting SIR solutions for long-time data including the cases of total and local alopecia (crosses, solid above) and for local alopecia alone (balls, solid below). Thin lines indicate the respective $I(t)$ in the SIR models. The large mean errors of $s = 75.83$ and $s = 36.98$ respectively, give strong reasons to doubt that the SIR model is appropriate to describe this disease.

can be interpreted as a parameter identification with additional weights for the mechanisms occurring in the model.

Regarding the particular Chernivtsi children disease, we have seen that the pure exponential growth and the SIR model of an epidemic provide a better fit to the observations and a better qualitative reproduction of the solution behavior than the simple contamination model, compare Fig. 1. So, we can estimate the model of pure exponential growth and the SIR model, describing rather an infection process, as more probable than the simple contamination model. Therefore, the presented investigation does not support the hypothesis in [12, 16].

Then, we have seen that the mean error between the model reproduction and the measurement data provides better approximation after the initial phase, which contains the most erroneous observations as already said in Section 2. So, it is the more appropriate quantitative criterion compared to exponential regression, which inversely weights the data.

At the same time, we have found that the reproduction ability does not imply a good prediction capability, i. e. the pure exponential growth, of course, cannot reproduce the saturation behavior of the number of infected persons. So, the inclusion of qualitative properties is a criterion while comparing models. The parameter identification of the SIR model generated a good reproduction of the quantitative data and a reproduction of the qualitative behavior. At the same time, the identified parameters predicted the observed total number of infected persons in the severe form rather well.

Since the SIR model is not able to reproduce the observations concerning the mild form with local alopecia, compare Fig. 3, we conclude that not all these mild cases are induced by a single and temporally well localized infection like the cases with the severe form do.

All together, we have seen that the combined model selection criterion including quantitative and qualitative aspects, allows rather strong implications by hands of a small number of observations. The analogous task of model selection and thus the detection of mechanisms reproducing the observed behavior, appears to be quite common in many life science applications.

Acknowledgement

This work was supported by the FP7-People-2011-IRSES project number 295164 (EUMLS: EU-Ukrainian Mathematicians for Life Sciences).

References

[1] N.T.J. Bailey, The Mathematical Theory of Epidemics, Griffin Book Co., London, 1957.

[2] K.P. Burnham, D.R. Anderson, Model Selection and Multimodel Inference: A Practical Information-Theoretic Approach, Springer, 2002.

[3] N.R. Draper, H. Smith, Applied Regression Analysis, John Wiley, New York, 1998.

[4] B. Göbel, M. Chung, K.M. Oltmanns, A. Peters, D. Langemann, Robust modeling of appetite regulation, J. Theor. Biol., 291 (2011) 65–75, doi 10.1016/j.jtbi.2011.09.012.

[5] International Atomic Energy Agency, The radiological accident in Goiania, Vienna, 1988, ISBN 92-0-129088-8.

[6] W.D. Kermack, A.G. McKendrick, A contribution to the mathematical theory of epidemics, J. Roy. Stat. Soc. Ser. A Gen. 115 (1927) 700-721, doi 10.1098/rspa.1927.0118.

[7] D. Langemann, L. Pellerin, A. Peters, Making sense of AMPA receptor trafficking by modeling molecular mechanisms of synaptic plasticity, Brain Res. 1207 (2008) 60–72, doi 10.1016/j.brainres.2008.01.097.

[8] D. Langemann, A. Peters, Deductive functional assignment of elements in the appetite regulation, J. Biol. Phys. 34 (2008) 413–424, doi 10.1007/s10867-008-9087-y.

[9] D. Langemann, M. Rehberg, Unbuffered and buffered supply chains in human metabolism, J. Biol. Phys. 36 (2010) 227–244, doi 10.1007/s10867-009-9178-4.

[10] J.D. Murray, Mathematical Biology I/II, Springer, New York, 2002.

[11] J. Nocedal, S. Wright, Numerical Optimization, Springer, New York, 2006.

[12] V.K. Patratii, G.I. Kokoshchuk, A.M. Bukharovich, L.A. Bezrukov, Chemical contamination syndrome in children with diffuse alopecia (in Russian), Pediatriia 12 (1991) 52–55, doi PubMed ID 1788021.

[13] W. Pschyrembel, Klinisches Wörterbuch (in German, Clinical dictionary), de Gruyter, Berlin, 2013.

[14] G. Schwarz, Estimating the dimension of a model, Ann. Statist. 6 (1978) 461–464.

[15] H. Stachowiak, Allgemeine Modelltheorie (in German, General model theorie), Springer, Berlin, 1973.

[16] V.K. Tatochenko, I.V. Koshel, G.A. Symsygina, A.G. Rumiantsev, A.M. Fedorov, I.E. Zykova, V.V. Liashko, T.F. Makarenko, M.D. Orel, E.B. Krolik, An epidemic outbreak of diffuse alopecia in children (in Russian), Pediatriia 12 (1990) 67–71, doi PubMed ID 2075067.

[17] H.R. Thieme, Mathematics in Population Biology, Univ. Press, Princeton, 2003.

[18] S. Tuljapurkar, H. Caswell, Structured-Population Models in Marine, Terrestrial, and Freshwater Systems, Springer, New York, 1997.

[19] P. Waltman, Deterministic Threshold Models in the Theory of Epidemics, Lecture Notes in Biomathematics **1**, Springer, Berlin, 1974.

[20] E.P. Wigner, The unreasonable effectiveness of mathematics in the natural sciences, Comm. Pure Appl. Math. 13 (1960) 1–14.

[21] D.D. Zerbino, L.N. Reznik, I.D. Babak, The results of a study of chemical-induced disease in children in Chernivtsi (in Russian), Vrach Delo 8 (1991) 88–91, doi Pub Med ID 1949748.

[22] D.D. Zerbino, A.M. Serdiuk, Chernivtsi Chemical Disease, New Ecologic Pathology? Essays about Epidemiology, Clinic Revealings, Ethiology, Versions of Genesis, Documents (in Ukrainian), Missioner, Lviv, 1998.

[23] http://emedicine.medscape.com/article/1069931-overview (2014) online cited 14/01/14.